Vector correlations in the photofragmentation of HN_3

K.-H. Gericke, R. Theinl, and F. J. Comes
Institut für Physikalische und Theoretische Chemie, Niederurseler Hang, D 6000 Frankfurt am Main 50, Federal Republic of Germany

(Received 7 December 1989; accepted 23 February 1990)

Hydrazoic acid was excited to its lowest electronic excited state $\tilde{A}\,^1A''$ and the fragments were analyzed by high resolution Doppler spectroscopy. The NH fragment is rotationally cold, while N_2 is strongly internally excited $f_{\rm int}(N_2) = 0.48$. The Λ doublets are populated statistically. The alignment of NH rotation vs the transition dipole moment of the parent is low ($\beta_{\mu J} < 0.14$). The vector correlation between the translational ($\mathbf{v}_{\rm NH}$) and rotational ($\mathbf{J}_{\rm NH}$) motion of the NH fragments is positive and increases with increasing $J_{\rm NH}$, indicating a preferential parallel alignment of $\mathbf{v}_{\rm NH}$ and $\mathbf{J}_{NH}$ ($\beta_{vJ} \simeq 0.40$). The observed correlation between the transition dipole moment of the parent and the NH($^1\Delta$) recoil velocity is negative at low NH rotations [$\beta_{\mu v}(J_{\rm NH} = 2) = -0.4$] and increases to positive values with increasing $J_{\rm NH}$. The HN_3 distorts from a nonplanar configuration after excitation of a linear-bent electronic transition in the NNN framework, resulting in a strong N_2 rotation and relatively weak NH rotation. The upper potential surface must be dependent on the torsional angle of the NN–NH system.

I. INTRODUCTION

The four atomic molecule hydrazoic acid is an interesting molecule for the study of the dynamics of a photofragmentation process because a double bond (N = N) is excited. Detailed investigations have been carried out at an excitation wavelength of 193 nm where most NH fragments are formed in their singlet states ($a\,^1\Delta$,$b\,^1\Sigma^+$, and $c\,^1\Pi$) and only a small part in the $A\,^3\Pi$ triplet state. The quantum yield for formation of NH($X\,^3\Sigma^-$) ground state products was found to be less than 0.2%, the detection limit of the experiment.[1]

The absorption spectrum of HN_3 in the region of its first maximum at 265 nm is entirely continuous with very small modulations,[2,3] indicating a fast dissociation process. The primary products NH and N_2 have been studied; but there may be another (minor) fragmentation channel where a hydrogen atom and a N_3 molecule are generated.[1,4,5] At 248 and 266 nm, the NH products are generated exclusively in the $a\,^1\Delta$ state[1,6] with low rotational excitation $f_R(\mathrm{NH}) = 3.7\%$ at 248 nm[1] and $f_R(\mathrm{NH}) = 3\%$ at 266 nm.[7] The nascent rotational product state distribution of NH($^1\Delta$, $v = 0$) produced by photolysis of HN_3 at 266 nm is a non-Boltzmann distribution peaking at $J_{\rm NH} = 5$–6.

In the present study, the photodissociation dynamics of hydrazoic acid has been analyzed under collision-free conditions by observation of scalar and vectorial properties of the NH product. The vector correlations between the transition dipole moment of HN_3 and the rotation, as well as the translation of the NH product, have been analyzed with sub-Doppler resolution since the quantitative determination of the $\langle \boldsymbol{\mu}\cdot\mathbf{J}\rangle$, $\langle \boldsymbol{\mu}\cdot\mathbf{v}\rangle$, $\langle \mathbf{v}\cdot\mathbf{J}\rangle$, and $\langle \boldsymbol{\mu}\cdot\mathbf{v}\cdot\mathbf{J}\rangle$ correlation gives a detailed picture of the fragmentation process.

II. EXPERIMENTAL

The scalar and vector properties in the photoexcitation of HN_3 were analyzed by sub-Doppler laser-induced fluorescence measurements of nascent NH products under different detection and polarization geometries. Details of the experimental setup have been published elsewhere.[7,8] In short, the photolysis pulse at 266 nm was delivered by a frequency quadrupled Nd:YAG laser (Quanta Ray, DCR 1) operating at a repetition rate of 10 Hz. The typical pulse energy was about 15 mJ at a pulse length of 6 ns. The NH products were probed by a frequency doubled dye laser (Lambda Physik, Fl 2002E) which was pumped by a second frequency doubled Nd:YAG laser (Spectron SL2 Q). The delay between both Nd:YAG lasers was kept constant at 30 ns with a time jitter below 5 ns.

The tuning range of the dye laser (308–330 nm) is sufficient to excite all rotational transitions of the (0,0) band of the NH ($c\,^1\Pi \leftarrow a\,^1\Delta$) electronic transition. The bandwidth of the dye laser in the UV was 0.1 cm^{-1} using a stepping motor tuned intracavity etalon. Both the photolyzing and the analyzing laser beams were linearly polarized and their planes of polarization can be rotated by $\lambda/2$ plates. The laser beam arrangement allowed experiments at three different probe geometries (geometry II, IV, and VI as defined in Ref. 9).

The undispersed fluorescence signal was viewed perpendicular to the laser beams regardless of polarization. The influence of scattered light was reduced by an interference filter [peak transmission at 327 nm with 10 nm full width at half-maximum (FWHM)]. For averaging and normalization to photolysis and analysis laser output energies, the signals were fed into a boxcar integrator (Stanford Research Systems, Model SR 250) and after A/D conversion stored in a micro computer (PC AT 386/7).

Hydrazoic acid was generated in a vacuum line using NaN_3 in excess of stearic acid.[10] When heated to 75–85 °C sufficient amounts of HN_3 evolved and were pumped directly into the observation cell. The HN_3 pressure was about 0.6 Pa controlled by a capacitance manometer for the observation of nascent NH products. For measurements in a supersonic jet, helium was bubbled through the NaN_3/stearic acid

 0021-9606/90/116548-08$03.00

mixture at a total pressure of 2×10^4 Pa. The pulsed nozzle with a diameter of 0.5 mm operated with a pulse length of less than 300 μs.[11]

III. RESULTS

The detailed knowledge of the correlated vector properties of a molecular photoproduct can provide a three-dimensional picture of the fragmentation process. Such experimental examinations in the dissociation of HN_3 were accomplished by the use of sub-Doppler polarization spectroscopy. The vectors of interest in these experiments are the HN_3 parent molecule transition dipole moment $\boldsymbol{\mu}$, the NH fragment recoil velocity vector $\mathbf{v}$, and the NH rotational angular momentum $\mathbf{J}$.

The theoretical framework required to convert the laboratory frame experiments of line profiles into the required bipolar moments that characterize the correlated ($\boldsymbol{\mu}$,$\mathbf{v}$,$\mathbf{J}$) distribution has been described by Dixon[12] for laser-induced fluorescence (LIF) and emission experiments. It has meanwhile been extended by Docker for $(n+m)$ LIF experiments[13] and by Mons and Dimicoli[14] for multiphoton ionization spectroscopy in connection with time-of-flight analysis of the ionized product. The fluorescence intensity for a single recoil velocity $v=\Delta\nu_D c/\nu_0$ can be expressed as a function of the relative Doppler shift $[x_D=(\nu-\nu_0)/\Delta\nu_D]$ from line center ν_0 in terms of bipolar moments.

$$I(x_D)=C\sum_{i=0}^{n} g_{2\cdot i}\cdot P_{2\cdot i}(x_D) \tag{1}$$

when linearly polarized photons are applied, where the possible value of i and the number of bipolar moments are determined by the number of photons n in the photolysis and the absorption fluorescence sequence [$n=3$ for conventional photolysis and $(1+1)$LIF analysis]. The terms $g_{2\cdot i}$ are linear combinations of bipolar moments $\beta_0^k(\mathbf{k}_1\mathbf{k}_2)$ which parametrize the ($\boldsymbol{\mu}$,$\mathbf{v}$,$\mathbf{J}$) correlations. The coefficients of these linear combinations depend on the polarization, the photolysis detection geometry, and the rotational branch which is used for analyzing the photoproducts.

Fortunately, one can simplify Eq. (1) for $(1+1)$ LIF according to Ref. 9 and neglect all but the first two terms in the line shape function. The line profile function[15]

$$I(x_D)\sim\frac{1}{\Delta\nu_D}[1+\beta_{\text{eff}}P_2(x_D)] \tag{2}$$

with $\beta_{\text{eff}}=g_2/g_0$ is fitted to the experimentally recorded Doppler line shapes with suitable convolution of the laser bandwidth, parent molecule translational motion, and N_2 velocity distribution. The N_2 velocity distribution is very well characterized by a Gaussian function which was determined by a high resolution pulsed dye laser system ($\Delta\nu_l=50$ MHz) when jet cooled HN_3 was photolyzed at 248 nm. The higher photolysis energy in that experiment in comparison to the 266 nm excitation should not significantly change the shape of the N_2 velocity distribution, since the same electronic transition is excited. Furthermore, the exact form of the velocity distribution does not strongly influence the line profile.

The anisotropy parameter β_{eff} contains information on the vector properties in the dissociation process

$$\beta_{\text{eff}}=[b_2\beta_{\mu\nu}+b_3\beta_{\nu J}+b_4\beta_{\mu\nu J}]/[b_0+b_1\beta_{\mu J}]. \tag{3}$$

The multipliers b_0–b_4 of the bipolar moments $\beta_{\mu J}$,$\beta_{\mu\nu}$, $\beta_{\nu J}$, and $\beta_{\mu\nu J}$ include the excitation detection geometry and angular momentum coupling factors. The numerical values of the multipliers b_0 to b_4 were calculated for P, Q, and R transitions and for the six different geometries I–IV defined in Ref. 10. The fact of observing undispersed fluorescence without using a polarizer has been taken into account. Transition probabilities were taken from the literature.[16,17]

We have measured the values of $\beta_{\text{eff}}(J_{\text{NH}})$ for three different geometries and for all nonoverlapping P, Q, and R transitions. The system of Eq. 3 was solved with a least-squares procedure and the bipolar moments and their rotational dependence were determined. In Figs. 1–4, the evaluated bipolar moments $\beta_{\mu J}$,$\beta_{\mu\nu}$,$\beta_{\nu J}$, and $\beta_{\mu\nu J}$ are shown as functions of J_{NH} within their theoretically defined range $-1\leqslant\beta_{\mu\nu J}\leqslant+0.5$ and $-0.5\leqslant\beta\leqslant+1.0$ for the remaining bipolar moments.

The alignment of the fragments, i.e., the correlation between $\boldsymbol{\mu}$ and $\mathbf{J}$, has only an indirect influence on the line profile. The integral of the line profile depends only on g_0:

$$\int I\,d\nu\sim g_0=b_0+b_1\beta_{\mu J}. \tag{4}$$

The value of $\beta_{\mu J}$, which is the renormalized rotational alignment parameter $A_0^{(2)}=\frac{4}{5}\beta_{\mu J}$, has been determined by measuring the integrated line intensities for different geometries and excitation branches. The rotational dependence of $\beta_{\mu J}$ is shown in Fig. 1. The NH($a\,^1\Delta$) products exhibit only a minor alignment in the photofragmentation at 266 nm which does not significantly change with fragment rotation. However, the positive values of $\beta_{\mu J}$ for all $J_{\text{NH}}>2$ indicate a preferentially parallel alignment between the transition dipole moment of the HN_3 and the rotational vector of the NH product.

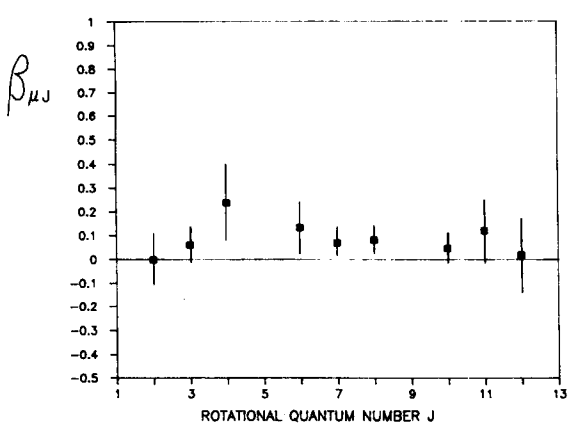

FIG. 1. Vector correlation between the transition dipole of the parent $\boldsymbol{\mu}$ and the rotational motion of the NH fragment $\mathbf{J}$ as a function of product rotation. The parameter $\beta_{\mu J}=\frac{1}{4}A_0^2$ was obtained by measuring the integrated line intensities for different geometries and excitation branches.

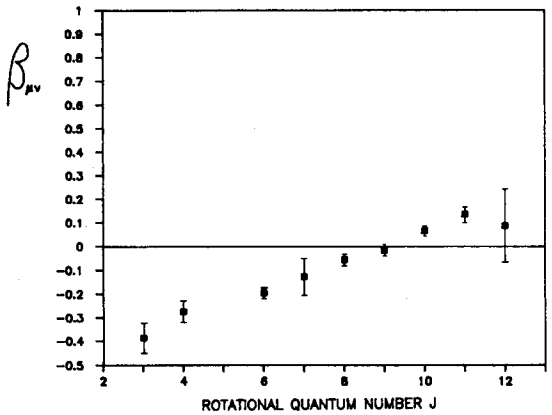

FIG. 2. Spatial anisotropy of NH fragments characterized by the bipolar moment $\beta_{\mu\nu} = \frac{1}{2}\beta$ as a function of J_{NH}.

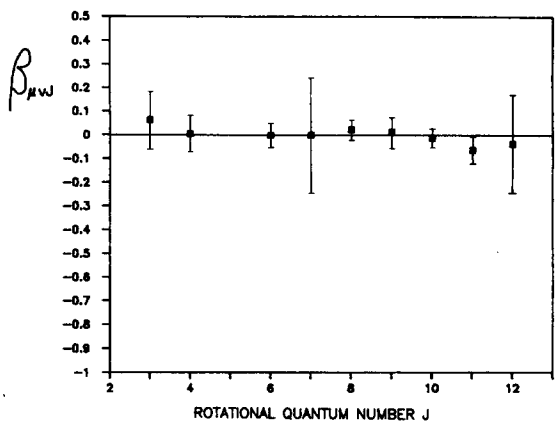

FIG. 4. Multiple vector correlation between μ, v, and J. The diminishing $\langle \mu \cdot v \cdot J \rangle$ correlation is a consequence of the low values for $\beta_{\mu J}$ and $\beta_{\nu J}$ at low J and of the low values for $\beta_{\mu J}$ and $\beta_{\mu\nu}$ at high J.

The influence of $\beta_{\mu J}$ on the evaluation of the other bipolar moments is not important because of its low value. The second bipolar moment $\beta_{\mu\nu}$ (Fig. 2) describes the spatial anisotropy of the photoproducts and is proportional to the classical anisotropy parameter $\beta = 2\beta_{\mu\nu}$. The negative value of $\beta_{\mu\nu}$ for the lowest rotational state $[\beta_{\mu\nu}(J_{NH} = 2) = -0.4]$ indicates a preferentially perpendicular alignment between μ and v. However, $\beta_{\mu\nu}$ increases with increasing J_{NH} and becomes positive for high product rotations ($J_{NH} > 9$).

The mutual correlation of the photofragment translational and rotational vector $\mathbf{v}_{NH}$ and $\mathbf{J}_{NH}$ is described by the bipolar moment $\beta_{\nu J}$. Since this moment is independent of the lab frame, $\beta_{\nu J}$ permits an insight into fragmentation dynamics directly in the molecular frame. Perfect alignment in the high J limit between v and J is given when $\beta_{\nu J} = +1$ or $\beta_{\nu J} = -0.5$ indicating that v is either parallel or perpendicular to J. We observe a positive $\langle v \cdot J \rangle$ correlation (Fig. 3) which increases with increasing J_{NH}. At high J, we obtain a value of $\beta_{\nu J} \simeq 0.40$ indicating the preference for a parallel alignment between v and J.

The last observed bipolar moment $\beta_{\mu\nu J}$ describes the mutual correlation between the HN_3 transition dipole moment μ, the translational, and the rotational motion of the NH fragment. Since only a low correlation between μ_{HN_3} and $\mathbf{J}_{NH}$ as well as between $\mu(_{HN_3})$ and $\mathbf{v}_{NH}$ for high J_{NH} is observed, a strong three vector correlation is not expected. Thus the low value of $\beta_{\mu\nu J}$ for all J_{NH} is not surprising (Fig. 4). We assume a value of $\beta_{\mu\nu J} = 0.0 \pm 0.05$ independent of fragment rotation.

IV. DISCUSSION OF THE DISSOCIATION PROCESS

The molecular structure of HN_3 in the electronic ground state is shown in Fig. 5. The planar HN_3 molecule consists of an almost linear N_3 chain ($\alpha_{NNN} = 171.3°$) and a strongly bent NH bond ($\alpha_{NNH} = 108.8°$). The NH distance in the HN_3 parent does not differ significantly from the $NH(^1\Delta)$ bond length of the free molecule $r_{NH} = 1.034$ Å. Also the bond length between the terminating nitrogen atoms is comparable with the $N_2(^1\Sigma_g^+)$ equilibrium distance $r_{NN} \simeq 1.098$ Å.

Near the ground state geometry $\tilde{X}\,^1A'$, only singlet states of A' or A'' geometry can be excited to a significant amount. The transition probability to the $^3A'$ or $^3A''$ states

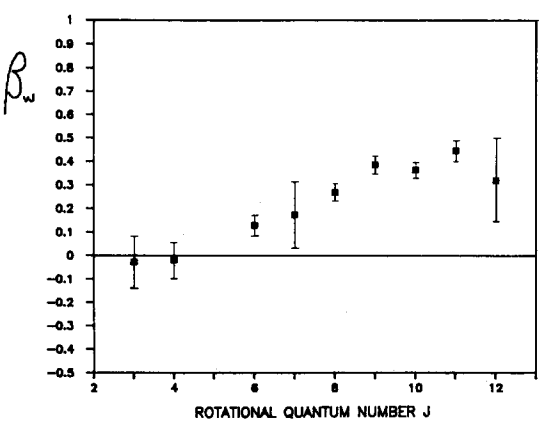

FIG. 3. Vector correlation between the translational v and rotational J motion of the NH fragment. The positive value of $\beta_{\nu J}$ indicates a preferentially parallel alignment between v and J. As a consequence, the NH rotation must be an out-of-plane motion of the initial planar HN_3 parent molecule.

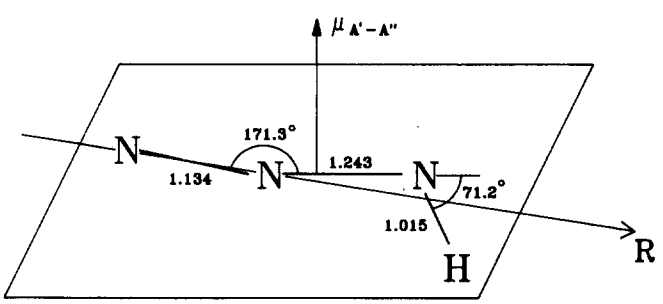

FIG. 5. Equilibrium configuration of the parent HN_3. The line between the centers-of-mass of NH of N_2 defines the R coordinate using a Jacobian coordinate system. The transition dipole moment μ for the lowest electronic transition $\tilde{A}\,^1D'' \leftarrow \tilde{X}\,^1A'$ is perpendicular to the symmetry plane of the parent (Ref. 19).

will be lower by several orders of magnitude. If we neglect the influence of the terminating H atom on the electronic transitions, then we expect two electronic excited states of $^1A'$ and $^1A''$ geometry both at the same energy. The transition moments to these states will be aligned perpendicular to the N_3 chain and in the molecular plane for one transition, but perpendicular to the plane for the other one. In this case, the photoexcitation of HN_3 will not strongly align the parent molecule in the lab frame and the ejected NH fragments should show a spatial isotropic distribution, i.e., a vanishing $\langle \mu \cdot v \rangle$ correlation with $\beta_{\mu v} = 0$. However, for the lowest rotational state of the $NH(^1\Delta)$ product, a value of $\beta_{\mu v} = -0.4$ is observed which is close to the theoretical limit of $\beta_{\mu v}(\max) = -0.5$ for a perfect perpendicular alignment between the transition dipole moment of the parent and the recoil velocity. Thus, only the $\tilde{A}\,^1A''$ state of HN_3 will be populated.

Ab initio calculations of Meier and Staemmler[18,19] demonstrate that five of the six singlet states ($3A'$ and $3A''$) of the HN_3 in its equilibrium geometry of the ground state correlate with $N_2(^1\Sigma_g^+)$ and different NH states: $NH(a\,^1\Delta)$ with $\tilde{X}\,^1A'$ and $\tilde{A}\,^1A''$, $NH(b\,^1\Sigma^+)$ with $\tilde{B}\,^1A'$, and $NH(c\,^1\Pi)$ with $\tilde{C}\,^1A'$ and $\tilde{D}\,^1A''$. In the photolysis of HN_3 at 248, 266, and 308 nm, all NH products are formed exclusively in the $a\,^1\Delta$ state.[1,20,21] Therefore, one would expect to excite only the $\tilde{A}\,^1A''$ state of the HN_3 parent molecule. Furthermore, the vertical excitation energies were calculated to be 4.96 eV for the $\tilde{A}\,^1A'' \leftarrow \tilde{X}\,^1A'$ transition and 6.57 eV for the $\tilde{B}\,^1A' \leftarrow \tilde{X}\,^1A'$ transition.[19] Experimentally, one observed 4.68 and 6.2 eV for the corresponding transitions.[3] Thus, at wavelengths $\geqslant 248$ nm, *only* the $\tilde{A}\,^1A''$ state will be excited and the transition dipole moment $\mu(\tilde{A}\,^1A'' \leftarrow \tilde{X}\,^1A')$ must be aligned *perpendicular* to the HN_3 plane (Fig. 5). At higher excitation energies ($\tilde{B}\,^1A' \leftarrow \tilde{X}\,^1A'$) also NH products in the $b\,^1\Sigma^+$ state can be generated as observed in the experiment at 193 nm.[1]

In order to discuss the origin of NH rotation, we will first consider the influence of initial vibrational motion of the parent. At room temperature, the NH stretch [$\nu_1(a') = 3336\ cm^{-1}$], the NNN asymmetric stretch [$\nu_2(a') = 2140\ cm^{-1}$], the NNN symmetric stretch [$\nu_3(a') = 1274\ cm^{-1}$], and the NNH bent [$\nu_4(a') = 1150\ cm^{-1}$] vibrational modes are not excited. Only the NNN in plane bent [$\nu_5(a') = 522\ cm^{-1}$] and the NNN out-of-plane bent [$\nu_6(a'') = 672\ cm^{-1}$] vibrational excited levels are populated to a small extent. The total initial vibrational energy of the parent $E_{vib}(HN_3, T = 300\ K) = 76\ cm^{-1}$ is negligibly small.

From all normal modes of HN_3, only zero point motion of the NNH ν_4 bending vibration can induce NH rotation. Zero point motion of the other modes will essentially be released as NH translation. If the upper potential surface of HN_3 ($\tilde{A}\,^1A''$) is only repulsive along the R coordinate (see Fig. 5) and does not induce any torque in the NH rotor, i.e., the anisotropy of the upper surface is zero, then the distribution of final rotational states $P(J)$ in the energy sudden approximation is determined by the expansion of the ground-state wave function $\Psi_{gr}(\gamma)$ in terms of the free rotor eigenstates $Y_{J_0}(\gamma,0)$[22]:

$$P(J) = |a_J|^2 / \sum_J |a_J|^2 \tag{5}$$

with the expansion coefficients

$$a_J = \langle \Psi_{gr} | Y_{J0} \rangle = 2\pi \int_0^\pi d\gamma \sin\gamma \Psi_{gr}(\gamma) Y_{J0}(\gamma,0). \tag{6}$$

Since the parent molecule is initially in its ν_4 vibrational ground state, the distribution of angles γ is a narrow Gaussian-type function centered at the NNH equilibrium angle $\gamma_0 = 108.8°$.

Using Jacobian coordinates, this angle will be transformed to an equilibrium angle of $\gamma_e = 113.5°$ for repulsion along the R coordinate. Figure 6 shows the calculated product state distribution (circles) in comparison to the experimental data squares. The electronic momentum of the $^1\Delta$ state is added to the nuclear motion. The pronounced structure of the calculated distribution [Eq. (5)] will vanish when the distribution of initial parent rotational states is taken into account.[23]

If final-state interaction is negligible, the product state distribution should be identical to that prepared in the first step. In the Franck–Condon limit, the final distribution is a direct reflection of the parent nuclear wave function. Since the observed product rotation is hotter than in the FC limit, final state interaction is responsible for the observed distribution.

The $\langle v \cdot J \rangle$ correlation contains detailed information about the origin of product rotation. We observe a positive β_{vJ} parameter which increases with increasing J_{NH} (Fig. 3). For high J, we assume it to be $\beta_{vJ} \cong +0.45$. It is well understood that an alignment between v and J strongly influences the Doppler line profile. For $v \| J$ the center of the Q lines will show increasing intensity in favor of the wings, whereas the P and R lines behave in just the opposite direction that the center of the lines decreases in intensity in favor of the wings. The reason for this behavior is the relation between the transition dipole moment μ of the product with the fragment rotation J. In the high J limit, μ is parallel to J for Q lines, whereas μ is perpendicular to J for P and R lines.

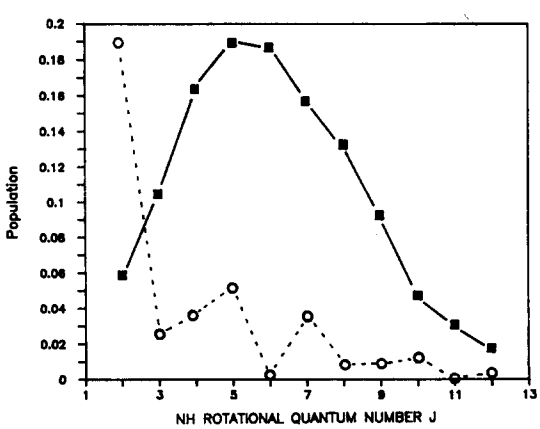

FIG. 6. Rotational product state distribution of $NH(a\,^1\Delta)$ in the photodissociation of HN_3 at 266 nm (filled squares). The circles represent the Franck–Condon limit without considering the electronic structure of $NH(^1\Delta)$.

In the one electron $\Sigma \leftarrow \Pi$ transitions, the Q transition probes one Λ doublet $\Pi(A'')$, while P and R lines probe the other Λ component $\Pi(A')$.[24] In the analysis of NH products, the two-electron $^1\Delta$ state is excited to a $^1\Pi$ state. Each rotational transition consists of a pair of lines. The initial level of one line is of $\Delta(A')$ symmetry, while the origin of the other line is the asymmetric $\Delta(A'')$ state. For an understanding of the line profiles, it is important to know the orientation of the transition dipole moment for these line pairs. In Fig. 7, the P, R, and Q branches for the NH $^1\Pi \leftarrow {}^1\Delta$ transition are shown. Right to the energy levels the symmetry of the electrons with respect to reflection of the spatial coordinates in the plane of rotation is shown.

The $\Delta(A')$ and $\Delta(A'')$ states are linear combinations of two π electrons which are identified by indices 1 and 2 in Fig. 7. The symmetry of Π states for a π^1 electron is directly given by its symmetry. π lobe in the plane of rotation for $^1\Pi(A')$ and π lobe parallel to J for $^1\Pi(A'')$.[24]

The possible transitions and the direction of the transition dipole moment μ is obtained by the matrix elements considering the parity rules $+ \rightarrow -, - \rightarrow +$:

$$\langle {}^1\Delta(A')|\mu(A'')|{}^1\Pi(A'')\rangle \equiv Q \text{ branch} \quad \mu \| \mathbf{J};$$
$$\langle {}^1\Delta(A')|\mu(A')|{}^1\Pi(A')\rangle \equiv P,R \text{ branch} \quad \mu \perp \mathbf{J};$$
$$\langle {}^1\Delta(A'')|\mu(A'')|{}^1\Pi(A')\rangle \equiv Q \text{ branch} \quad \mu \| \mathbf{J};$$
$$\langle {}^1\Delta(A'')|\mu(A')|{}^1\Pi(A'')\rangle \equiv P,R \text{ branch} \quad \mu \perp \mathbf{J}. \qquad (7)$$

Here $\mu(A'')$ represents a transition dipole moment perpendicular to the plane of rotation and $\mu(A')$ is the transition moment in the plane of rotation. The other transitions are forbidden:

$$\langle {}^1\Delta(A')|\mu(A')|{}^1\Pi(A'')\rangle$$
$$= \langle {}^1\Delta(A')|\mu(A'')|{}^1\Pi(A')\rangle$$
$$= \langle {}^1\Delta(A'')|\mu(A'')|{}^1\Pi(A'')\rangle$$
$$= \langle {}^1\Delta(A'')|\mu(A')|{}^1\Pi(A')\rangle = 0.$$

Thus both transition dipole moments for the Q lines probing different Λ levels are parallel to J and the transition dipole moments for P and R lines are perpendicular to J. In the analysis of the Doppler profile, both Λ levels are treated equally and the observed vector correlations as a function of product rotation represent the average of the $^1\Delta(A')$ and $^1\Delta(A'')$ states.

Since we observe a dip in the line profiles of P or R lines and an increased intensity in the center of the line when Q transitions are excited, v and J are aligned preferentially parallel to one another. In the high J limit, the average angle θ_{vJ} between v and J is given by

$$\beta_{vJ} = \langle P_2(\cos\theta_{vJ})\rangle.$$

With $\beta_{vJ} = +0.40$, we obtain an average angle of $\langle\theta_{vJ}\rangle \cong 39°$. If the influence of initial parent rotation on the dissociation dynamics is negligible, then a parallel alignment between the translational and rotational motion of the NH product can only be generated by a torsional motion of the NH–N_2 system due to conservation of angular momentum.

The fraction of rotational energy induced by torsion $f_{\text{torsion}} = \langle E_{\text{torsion}}\rangle/E_{\text{rot}}$, or bending motion $f_{\text{bend}} = \langle E_{\text{bend}}\rangle/E_{\text{rot}}$ is given by

$$f_{\text{torsion}} = (1 + 2\beta_{vJ})/3 \cong 60\%,$$
$$f_{\text{bend}} = 2(1 - \beta_{vJ})/3 \cong 40\%. \qquad (8)$$

Thus the major part of rotational energy is induced by a nonplanar (torsional) motion of the NH rotor during the fragmentation process.

The influence of parent rotation on J_{NH} can be estimated by simple classical calculation where parent rotation about the three axes of inertia will be transferred into fragment internal rotation or orbital angular momentum. In the case of HN_3 ($kT/2 = 104\,\text{cm}^{-1}$ for each degree of freedom), $J_{\|} = 2.2\,\hbar$ will be transferred into NH rotation where the rotational vector is aligned along the recoil R axis and $J_{\perp} = 0.4\,\hbar$ for a perpendicular alignment between v and J. Since much more product rotation is generated in the dissociation process (see Fig. 6), the observed positive $\langle \mathbf{v}\cdot\mathbf{J}\rangle$ correlation is not caused by parent rotation, but mainly by the dynamics of the fragmentation process. This is confirmed by the analysis of Doppler broadened NH lines in the photodissociation of HN_3 at 248 nm in a molecular beam, where the initial parent motion is significantly reduced to a rotational energy of less than 10 K. Since in this beam experiment a positive $\langle \mathbf{v}\cdot\mathbf{J}\rangle$ correlation is also observed, the product rotation must be generated via a nonplanar motion of the NH rotor.

Another hint for the nonplanarity of the dissociation process is the population of the Λ doublets. HN_3 is excited to the $\tilde{A}\,{}^1A''$ state which has an antisymmetric wave function

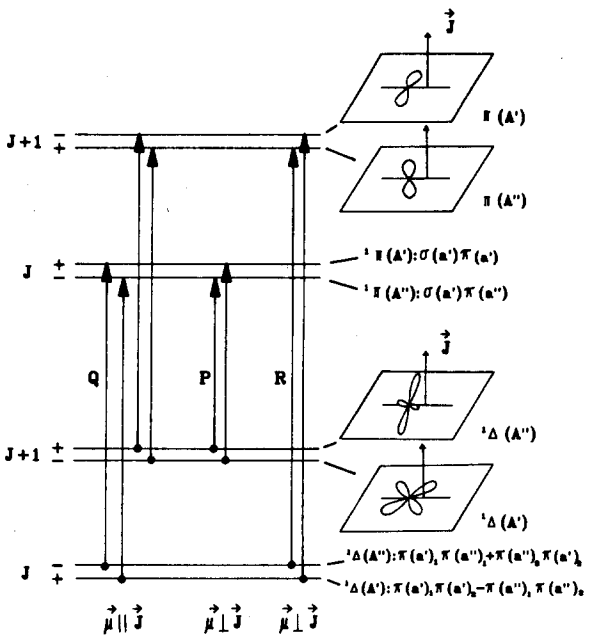

FIG. 7. P, Q, and R branches in the $^1\Pi \leftarrow {}^1\Delta$ system. The energy splitting in the Λ doublets is much larger in the Π state than in the Δ state. The symmetry of the Λ doublets is shown to the right of each level. The wave function of the upper Λ component of the Π system and of the lower Λ level of the Δ system is symmetric with respect to reflection of the spatial coordinates of the electrons on the plane of rotation, while the wave functions of the other Λ components are antisymmetric. Each transition consists of a pair of lines and the transition moment μ of each line lies parallel to J for the Q branch, but perpendicular to J for the P and R branches. The parity of the levels is given for even J.

with respect to reflection in the molecular plane. For a planar fragmentation, i.e., the N_2 and NH bond will always lie in this plane, the wave function of the NH fragment should also be antisymmetric with respect to reflection, since the wave funcion of the $N_2(X\,^1\Sigma_g^+)$ is symmetric. Thus, the $\Delta(A'')$ levels of the $NH(a\,^1\Delta)$ product should be preferentially populated, because the wave function of this state is antisymmetric (Fig. 7). However, no preferred population has been found within the experimental error of 10%.[7]

While the vector correlation between $\mathbf{v}$ and $\mathbf{J}$ is independent of the dissociation lifetime, since $\mathbf{v}$ and $\mathbf{J}$ are only produced at the moment of fragmentation, the vector correlation between the transition dipole of the parent $\boldsymbol{\mu}$ and the recoil velocity $\mathbf{v}$ depend on the time scale of the dissociation process for a rotating parent, since $\boldsymbol{\mu}$ is aligned with $\mathbf{E}$, the electric field vector of the photolyzing laser beam, at $t=0$, but the velocity is determined at the moment of separation and is analyzed for a period of time much longer than the fragmentation lifetime

$$\beta_{\mu v} = \langle P_2(\boldsymbol{\mu}_{t=0} \cdot \mathbf{v}_{t=\infty}) \rangle. \tag{9}$$

Only the $\tilde{A}\,^1A'' \leftarrow \tilde{X}\,^1A'$ electronic transition is excited, where the transition dipole moment is perpendicular to the plane of the parent.[18,19] If this planar geometry is conserved during the fragmentation process, $\beta_{\mu v}$ should be negative (and close to -0.5) for all product rotations. However, the observed increase of the $\langle \boldsymbol{\mu} \cdot \mathbf{v} \rangle$ correlation with increasing fragment rotation to positive values implies a motion of the direction $\mathbf{R}$ towards the $\mathbf{E}$ vector during fragmentation. Since $\boldsymbol{\mu}$ is perpendicular to the initial plane of the parent HN_3 molecule, this motion corresponds to an out-of-plane wagging vibration comparable to the $\nu_6(a'')$ mode. Thus a linear-bent electronic transition in the NNN frame is excited and the HN_3 distorts from a NN–NH bent configuration.

A pictorial view of the photofragmentation of hydrazoic acid is shown in Fig. 8. The NNN frame is bent and the direction of repulsion is given by the dissociation coordinate $\mathbf{R}$. The average angle of $\theta_{\mu v} = 49.8°$ is calculated from the observed $\beta_{\mu v}$ value at high NH rotations $\beta_{\mu v} = \langle P_2(\cos\theta_{\mu v}) \rangle$.

Since the mass of the terminating hydrogen atom is much lower than that of the nitrogen atoms, the bending vibration is essentially determined by the NNN framework. Consequently, the N_2 fragment should exhibit a much higher rotational excitation than the NH fragment. The internal energy of the N_2 product can be measured by $(2+2)$ REMPI, or by an accurate measurement of the velocity v_{NH} of the NH partner fragment which is generated in the same dissociation process[26]

$$E_{\text{int}}(N_2) = E_{\text{av}} - E_{\text{int}}(NH) - \tfrac{1}{2} m_{NH}^2 v_{NH}^2 / \mu_{N_2NH}, \tag{10}$$

in which E_{av} is the available energy and $\mu_{N_2\text{-}NH}$ is the reduced mass of the N_2–NH system. Figure 9 shows the mean internal energy of the N_2 partner fragment as a function of NH rotation obtained by linewidth measurements of the $c\,^1\Pi \leftarrow a\,^1\Delta$ transitions. Final resolution of the dye laser and residual Doppler motion of the parent has been considered. The internal energy of the N_2 product shows only a minor dependence on the rotation of the NH fragment. The average value of internal N_2 energy is extremely high $\langle E_{\text{int}}(N_2) \rangle = 9900\ \text{cm}^{-1}$.

The exact shape of the N_2 internal energy distribution could not be determined because of the remaining HN_3 Doppler motion, the resolution of the dye laser, and the narrow energy spacing of N_2 rotational quantum states. However, high resolution experiments ($\Delta\nu_l \lesssim 50$ MHz) in a molecular beam at a photolysis wavelength of 248 nm show no structure in the line profile which is to be interpreted as N_2 vibrational energy. Therefore, we conclude that in the photodissociation of HN_3 at 266 nm, the N_2 products are generated with extremely high rotational excitation. The product state distribution is fitted to a Gaussian distribution. The average rotational energy of 9900 cm^{-1} corresponds to a mean N_2 rotation at quantum number of $\langle J_{N_2} \rangle = 70$. The width ΔJ of the rotational state distribution $P(J_{N_2})$ is determined by the width of the fitted Gaussian velocity distribution

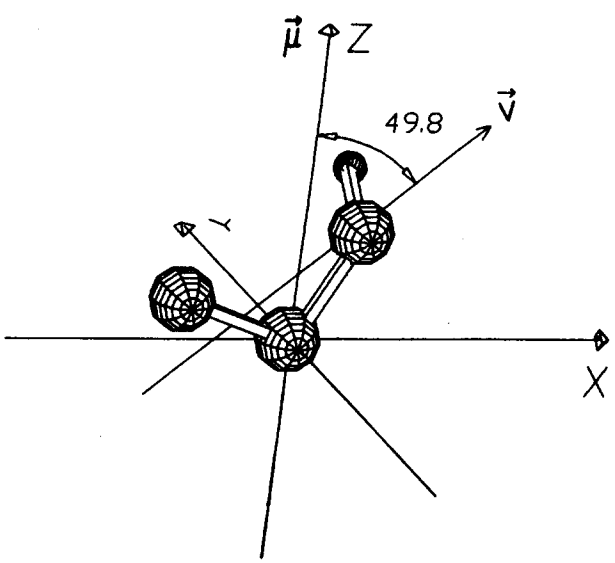

FIG. 8. A pictorial view of the fragmentation of hydrazoic acid at 266 nm. A linear-bent electronic transition within the NNN frame is excited and HN_3 becomes distorted from a strongly bent configuration.

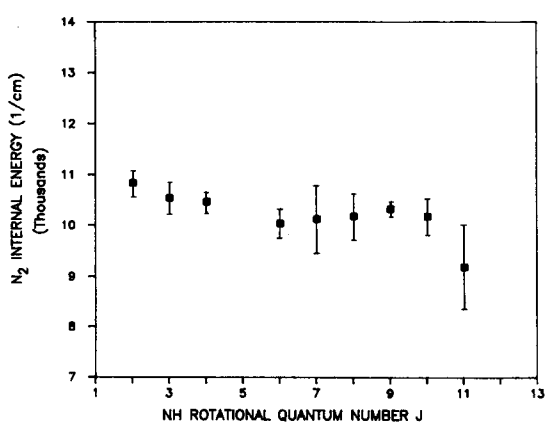

FIG. 9. Mean internal energy of the N_2 partner product as a function of NH rotation.

$$P(J_{N_2}) \sim \exp\left[-\left(\frac{J-\langle J_{N_2}\rangle}{\Delta J}\right)^2 4\ln 2\right] \quad (11)$$

with $\Delta J = 15$ (FWHM).

These observations are supported by the results of (2 + 2) REMPI measurements performed by Dagdigian and co-workers[25] where high power laser beams ~283 nm were used to photolyze HN_3 and to analyze the N_2 product through its $a\ ^1\Pi$ state with the same light pulse. The N_2 products were found to be vibrationally cold, but highly rotationally excited with an average rotational excitation of ~6.400 cm^{-1}. A lower rotational excitation in the REMPI work can be expected since a lower HN_3 excitation energy is used. The N_2 product state distribution in the photodissociation of HN_3 at 283 nm is roughly Gaussian shaped with the most probable N_2 rotation at $\langle J_{N_2}\rangle = 56$ and a width of $\Delta J = 13$–14 (FWHM).[25] The results at 283 and 266 nm photolysis wavelength indicate that the increase of HN_3 excitation energy will essentially be transferred into N_2 rotation.

A rough estimation of the lifetime of the dissociation process can be extracted from the $\beta_{\mu v}$ value at the lowest rotational state. We start with the model assumption that the parent molecule become distorted in a plane. For an instantaneous planar dissociation with μ perpendicular to the molecular plane the limiting value of $\beta_{\mu v} = -0.5$ is expected. A deviation from this value can be attributed to a deflection of the recoil velocity by the tangential velocity v_t of the rotating parent and to a HN_3 rotation through an angle $\delta = \omega \cdot \tau$ before fragmentation where ω describes the angular velocity and τ the lifetime of the parent in the excited state.[27] Since the tangential velocity is very small ($v_t \cong 290$ m/s) in comparison to the recoil velocity ($v \cong 3300$ m/s), the value of $\beta_{\mu v}$ is reduced mainly by the finite time of dissociation (angle of deflection $\simeq 5°$). Following the work of Bush and Wilson,[27] we obtain for a first order decay the upper limit for the fragmentation time $\tau \leqslant 100$ fs. This short dissociation time on the femtosecond time scale is in accordance with the broad and only weakly modulated HN_3 absorption spectrum. However, the value of τ can only be interpreted as an upper limit because the strong NNN bending motion mainly influences the $\beta_{\mu v}$ parameter as can be seen for high NH product rotations where $\beta_{\mu v}$ becomes positive (Fig. 2). As a consequence, the dissociation geometry becomes dependent on the dissociation lifetime. This can also be seen when the ratio of the $\langle \mu \cdot v \rangle$ and the $\langle \mu \cdot J \rangle$ correlation is considered. Corresponding to Eq. (9) $\beta_{\mu J}$ can be written in the classical limit

$$\beta_{\mu J} = \langle P_2(\mu_{\tau=0} \cdot J_{\tau=\infty}) \rangle. \quad (12)$$

Following the work of Docker *et al.*[28] and the azimuthally averaged addition theorem described by Barnwell *et al.*[29] we can separate the complete fragmentation process into two parts, one part before dissociation has started (up to time τ) and the other part after dissociation has begun:

$$\beta_{\mu J} = \langle P_2(\mu_{t=0} \cdot \mu_{t=\tau}) P_2(\mu_{t=\tau} \cdot J_{t=\infty}) \rangle; \quad (13)$$

$$\beta_{\mu v} = \langle P_2(\mu_{t=0} \cdot \mu_{t=\tau}) P_2(\mu_{t=\tau} \cdot v_{t=\infty}) \rangle. \quad (14)$$

If the dissociation geometry is *independent* of the fragmentation lifetime, then the ratio of the two expressions cancels the lifetime factor

$$\frac{\beta_{\mu J}}{\beta_{\mu v}} = \frac{\langle P_2(\mu_{t=\tau} \cdot J_{t=\infty}) \rangle}{\langle P_2(\mu_{t=\tau} \cdot v_{t=\infty}) \rangle}. \quad (15)$$

This "geometry index" $\beta_{\mu J}/\beta_{\mu v}$[28] should be approximately independent of the lifetime if the dissociation geometry is independent of the time of separation. Since we observe a low $\beta_{\mu J}$ value independent of J_{NH}, but a strongly increasing $\beta_{\mu v}$ parameter with increasing J_{NH}, the fragmentation geometry should depend on the dissociation lifetime.

From the knowledge of the $NH(^1\Delta)$ and $N_2(^1\Sigma_g^+)$ product pair rotation information about the orbital angular momentum $L_{N_2\text{-}NH}$ and the impact parameter b can be extracted. In general, conservation of angular momentum limits the range of the orbital angular momentum for a nonrotating HN_3 parent to

$$J_{N_2} + J_{NH} \geqslant L_{N_2\text{-}NH} \geqslant |J_{N_2} - J_{NH}|. \quad (16)$$

Furthermore, the available phase space is also limited by energy conservation

$$L_{N_2\text{-}NH} = b\sqrt{2\mu_{N_2\text{-}NH}\left[E_{av} - E_{rot}(N_2) - E_{rot}(NH)\right]}, \quad (17)$$

where the relation

$$L_{N_2\text{-}NH} = \mu_{N_2\text{-}NH}\, b v_{N_2\text{-}NH} \quad (17)$$

is used, with $v_{N_2\text{-}NH}$ being the relative velocity of the products N_2 and $NH(^1\Delta)$.

Since the NH partners exhibit only low rotational excitation and the N_2 fragments are formed with high rotation [even for a nonrotating $NH(^1\Delta)$ partner fragment at $J_{NH} = 2$, see Fig. 9], the orbital angular momentum is essentially characterized by N_2 rotation.[30] For $L_{N_2\text{-}NH} \cong \langle J_{N_2}\rangle = 70\,\hbar$ and $v_{NH} = 3300$ m/s, we obtain an impact parameter of $b \cong 0.9$ Å which is not strongly dependent on J_{NH} rotation. This impact parameter is larger than the distance between the N_2 center-of-mass and the HN_3 center-of-mass in its equilibrium position ($d = 0.64$ Å). A completely different situation is observed in the photodissociation of H_2O_2, where the rotational vectors of the OH products are oriented essentially in the opposite direction and an extremely low value for the orbital angular momentum is observed.[11]

The range of the impact parameter Δb is essentially given by the spread of the observed recoil velocity and one obtains $\Delta b \cong 0.26$ Å. The correlation of product quantum states as indicated in Fig. 9 gives some further hints on the impact parameter distribution. If more energy is released into internal product excitation, the translational energy slightly decreases (Fig. 9). If b is constrained, a lower velocity of $v_{N_2\text{-}NH}$ results in less orbital angular momentum [Eq. (17)] and therefore in less N_2 rotation $L_{N_2\text{-}NH} \approx |J_{NH} + J_{NH}|$. In this case, rotationally excited NH products correlate with N_2 partner fragments in lower rotational states.

ACKNOWLEDGMENTS

This research was supported by a Schwerpunkt program of the Deutsche Forschungsgemeinschaft. We thank Professor V. Staemmler and Dr. U. Meier for stimulating discussions and for sending results of their calculations prior

to publication. We are grateful for the receipt of preliminary results of the N_2-REMPI measurements from Professor P. J. Dagdigian. We also thank T. Haas for his cooperative assistance in part of the measurements.

[1]F. Rohrer and F. Stuhl, J. Chem. Phys. **88**, 4788 (1988).
[2]H. Okabe, J. Chem. Phys. **49**, 2726 (1968).
[3]J. R. McDonald, J. W. Rabalais, and S. P. McGlynn, J. Chem. Phys. **52**, 1332 (1970).
[4]R. S. Konar, S. Mabunoto, and B. de BDarwent, Trans. Faraday Soc. **67**, 1698 (1971).
[5]A. Sevin, J. P. Le Roux, P. Bigot, and A. Devaquet, Chem. Phys. **45**, 305 (1980).
[6]J. R. McDonald, R. G. Miller, and A. P. Baronavski, Chem. Phys. Lett. **51**, 57 (1977).
[7]K.-H. Gericke, R. Theinl, and F. J. Comes, Chem. Phys. Lett. **164**, 605 (1990).
[8]A. U. Grunewald, K. -H. Gericke, and F. J. Comes, J. Chem. Phys. **87**, 5709 (1987).
[9]K.-H. Gericke, S. Klee, F. J. Comes, and R. N. Dixon J. Chem. Phys. **85**, 4463 (1986).
[10]B. Krakow, R. C. Lord, and G. O. Neely, J. Mol. Spectrosc. **27**, 148 (1986).
[11]K.-H. Gericke, H. G. Gläser, C. Maul, and F. J. Comes, J. Chem. Phys. **92**, 415 (1990).
[12]R. N. Dixon, J. Chem. Phys. **85**, 1866 (1986).
[13]M. P. Docker, Chem,. Phys. **135**, 405 (1989).
[14]M. Mons and I. Dimicoli, J. Chem. Phys. **90**, 4037 (1989).
[15]This parameter β_{eff} incorporates already the term $P_2(\cos\theta)$ which sometimes is written explicitly in the line profile function (Ref. 9).
[16]J. M. Lents, J. Quantum Spectrosc. Radiat. Transfer **13**, 297 (1973).
[17]R. Rohrer, dissertation, Universität Bochum, 1987.
[18]V. Staemmler and U. Meier (private communication).
[19]U. Meier, dissertation fakultät für chemie an der Ruhr-Universität Bochum, 1988.
[20]A. P. Baronavski, R. G. Miller, and J. R. McDonald, Chem. Phys. **30**, 119 (1978).
[21]K.-H. Gericke, M. Lock, and F. J. Comes (to be published).
[22]R. Schinke, J. Phys. Chem. **90**, 1743 (1986).
[23]P. Andresen and R. Schinke, in *Molecular Photodissociation Dynamics*, edited by M. N. R. Ashfold and J. E. Baggott (The Royal Society of Chemistry, London, 1987).
[24]M. H. Alexander, P. Andresen, R. Bacis, R. Bersohn, F. J. Comes, P. J. Dagdigian, R. N. Dixon, R. W. Field, G. W. Flynn, K.-H. Gericke, E. R. Grant, B. J. Howard, J. R. Huber, D. S. King, J. L. Kinsey, K. Kleinermanns, K. Kuchitsu, A. C. Luntz, A. J. McCaffery, B. Pouilly, H. Reisler, S. Rosenwaks, E. W. Rothe, M. Shapiro, J. P. Simons, R. Vasudev, J. R. Wiesenfeld, C. Wittig, and R. N. Zare, J. Chem. Phys. **89**, 1749 (1988).
[25]P. J. Dagdigian (private communication).
[26]K.-H. Gericke, Phys. Rev. Lett. **60**, 561 (1988).
[27]G. E. Bush and K. R. Wilson, J. Chem. Phys. **56**, 3638 (1972); **56**, 3655 (1972); C. Jonah, *ibid.* **55**, 1915 (1971).
[28]M. P. Docker, A. Ticktin, U. Brühlmann, and J. R. Huber, J. Chem. Soc. Faraday. Trans. 2 **85**, 1169 (1989).
[29]J. D. Barnwell, J. G. Loeser, and D. R. Herschbach, J. Phys. Chem. **87**, 2781 (1983).
[30]Transfer of initial parent rotation into N_2 product rotation is also negligible, because from classical calculations one concludes that less than five quanta of HN_3 rotation (essentially from the A and B axis of inertia) will be found as N_2 rotation.